Supplementary information for

‘TEMPERATURE-SENSITIVE REACTION INTERMEDIATE OF F_1-ATPASE’

Rikiya Watanabe[1], Ryota Iino[2], Katsuya Shimabukuro[3], Masasuke Yoshida[4], Hiroyuki Noji[2]
From the [1] Department of Mechanical Engineering, The University of Tokyo, Tokyo 113-8656, Japan, and [2]Institute of Scientific and Industrial Research, Osaka University, Ibaraki 567-0047, Japan, and [3]Florida State University, Tallahassee, Florida 32306-4370, USA, and [4]Chemical Resources Laboratory, Tokyo Institute of Technology, Yokohama 226-8603, Japan

1. Kinetic analysis of the dwell time distributions

➢ Scheme 1 *TS reaction is ADP release*

Here we assume that TS reaction is ADP release and that it follows ATP binding. The reaction scheme is given by

$$F_1 \bullet ADP \xrightarrow{k_{on}^{ATP}[ATP]} ATP \bullet F_1 \bullet ADP \underset{k_{on}^{ADP}[ADP]}{\overset{k_{TS}(=k_{off}^{ADP})}{\rightleftarrows}} ATP \bullet F_1 \xrightarrow{k_{rot}} ATP \bullet F_1^* \qquad (*1)$$

where k_{off}^{ADP}, k_{on}^{ADP}, k_{on}^{ATP}, and k_{rot} are the rate constants of ADP release (= the temperature sensitive reaction k_{TS}, (7.2 s^{-1})), ADP rebinding, ATP binding, and mechanical rotation, respectively. According to the experimental data (Fig. 2A, S3A), k_{on}^{ATP}, k_{on}^{ADP} were determined to be 9.9 x 10^4 $M^{-1}s^{-1}$, 1.7 x 10^5 $M^{-1}s^{-1}$, respectively. The rate constant of k_{rot} was determined to be 8.5 x 10^2 s^{-1} (for 10 degrees angle rotation) from a high speed imaging of the rotation of magnetic beads. Then, differential equations for the probabilities of F_1 in each chemical state are given as follows:

$$\frac{d[F_1 \cdot ADP]}{dt} = -k_{on}^{ATP}[\mathrm{ATP}][F_1 \cdot ADP] \qquad (*2)$$

$$\frac{d[ATP \cdot F_1 \cdot ADP]}{dt} = k_{on}^{ATP}[\mathrm{ATP}][F_1 \cdot ADP] - k_{TS}[ATP \cdot F_1 \cdot ADP] + k_{on}^{ADP}[\mathrm{ADP}][ATP \cdot F_1] \qquad (*3)$$

$$\frac{d[ATP \cdot F_1]}{dt} = k_{TS}[ATP \cdot F_1 \cdot ADP] - (k_{on}^{ADP}[\mathrm{ADP}] + k_{rot})[ATP \cdot F_1] \qquad (*4)$$

$$\frac{d[ATP \cdot F_1^*]}{dt} = k_{rot}[ATP \cdot F_1] \qquad (*5)$$

Initial conditions of $[F_1 \cdot ADP]$ and $[ATP \cdot F_1 \cdot ADP]$ are as follows:

$[F_1 \cdot ADP] = 100\%$, $[ATP \cdot F_1 \cdot ADP] = 0\%$ at t = 0

Simultaneous differential equations (*2~*5) were solved, and [$ATP \cdot F_1$] is expressed by

$$[ATP \cdot F_1] = \delta\{(\gamma-\beta)e^{\alpha t} + (\alpha-\gamma)e^{\beta t} + (\beta-\alpha)e^{\gamma t}\} \quad (*6)$$

$$\alpha = -k_{on}^{ATP}[\mathrm{ATP}]$$

$$\beta = \{-(k_{TS} + k_{on}^{ADP}[\mathrm{ADP}] + k_{rot}) + \sqrt{-4k_{TS}k_{rot} + (k_{TS} + k_{on}^{ADP}[\mathrm{ADP}] + k_{rot})^2}\}/2$$

$$\gamma = \{-(k_{TS} + k_{on}^{ADP}[\mathrm{ADP}] + k_{rot}) - \sqrt{-4k_{TS}k_{rot} + (k_{TS} + k_{on}^{ADP}[\mathrm{ADP}] + k_{rot})^2}\}/2$$

$$\delta = \frac{100\alpha k_{TS}}{(\gamma-\beta)(\beta-\alpha)(\alpha-\gamma)}$$

The histogram of the dwell time between steps corresponds to the differentiation of [$ATP \cdot F_1$*]. The observed dwell time distributions were simulated according to the solved equation (*7). The reproduced data was shown as red lines in Fig.S1.

$$\frac{d[ATP \cdot F_1^*]}{dt} = k_{rot}\delta\{(\gamma-\beta)e^{\alpha t} + (\alpha-\gamma)e^{\beta t} + (\beta-\alpha)e^{\gamma t}\}\} \quad (*7)$$

➢ **Scheme 2 *TS reaction is NOT ADP release***

Here we assume that ADP release is not TS reaction, and that ADP release occurs after ATP binding and TS reaction. The kinetic scheme is given by

$$F_1 \bullet ADP \xrightarrow{k_{on}^{ATP}[ATP]} ATP \bullet F_1 \bullet ADP \xrightarrow{k_{TS}} ATP \bullet F_1^{\#} \bullet ADP \underset{k_{on}^{ADP}[ADP]}{\overset{k_{off}^{ADP}}{\rightleftharpoons}} ATP \bullet F_1^{\#} \xrightarrow{k_{rot}} ATP \bullet F_1^* \quad (*8)$$

where k_{TS}, k_{on}^{ATP}, k_{rot} are 7.2 s^{-1}, 9.9 x 10^4 $M^{-1}s^{-1}$, 8.5 x 10^2 s^{-1}, respectively. k_{off}^{ADP} / k_{on}^{ADP} was fixed at 4.3 x 10^{-5} M according to the experimentally determined value of K_i^{ADP} (Fig.S3A). The differential equations of the probability of F_1 in each chemical state are given by

$$\frac{d[F_1 \cdot ADP]}{dt} = -k_{on}^{ATP}[\mathrm{ATP}][F_1 \cdot ADP] \quad (*9)$$

$$\frac{d[ATP \cdot F_1 \cdot ADP]}{dt} = k_{on}^{ATP}[\mathrm{ATP}][F_1 \cdot ADP] - k_{TS}[ATP \cdot F_1 \cdot ADP] \quad (*10)$$

$$\frac{d[ATP \cdot F_1^{\#} \cdot ADP]}{dt} = k_{TS}[ATP \cdot F_1 \cdot ADP] - k_{off}^{ADP}[ATP \cdot F_1^{\#} \cdot ADP] + k_{on}^{ADP}[\mathrm{ADP}][ATP \cdot F_1^{\#}] \quad (*11)$$

$$\frac{d[ATP \cdot F_1^{\#}]}{dt} = k_{off}^{ADP}[ATP \cdot F_1^{\#} \cdot ADP] - (k_{on}^{ADP}[\mathrm{ADP}] + k_{rot})[ATP \cdot F_1^{\#}] \quad (*12)$$

$$\frac{d[ATP \cdot F_1{}^*]}{dt} = k_{rot}[ATP \cdot F_1^{\#}] \quad (*13)$$

Initial conditions of $[F_1 \cdot ADP]$ and $[ATP \cdot F_1 \cdot ADP]$ are as follows:

$[F_1 \cdot ADP] = 100\%$, $[ATP \cdot F_1 \cdot ADP] = 0\%$ at t = 0

Simultaneous differential equation (*9~*13) can be solved, and $[ATP \cdot F_1^{\#}]$ is expressed by

$$[ATP \cdot F_1^{\#}] = \varepsilon\{(\delta-\gamma)(\beta-\gamma)(\beta-\delta)e^{\alpha t} + (\delta-\gamma)(\alpha-\gamma)(\alpha-\delta)e^{\beta t} + (\beta-\alpha)(\alpha-\delta)(\beta-\delta)e^{\gamma t} + (\beta-\alpha)(\alpha-\gamma)(\beta-\gamma)e^{\delta t}\} \quad (*14)$$

$$\alpha = -k_{on}^{ATP}[\mathrm{ATP}]$$

$$\beta = -k_{TS}$$

$$\gamma = \{-(k_{off}^{ADP} + k_{on}^{ADP}[\mathrm{ADP}] + k_{rot}) - \sqrt{-4k_{off}^{ADP}k_{rot} + (k_{off}^{ADP} + k_{on}^{ADP}[\mathrm{ADP}] + k_{rot})^2}\}/2$$

$$\delta = \{-(k_{off}^{ADP} + k_{on}^{ADP}[\mathrm{ADP}] + k_{rot}) + \sqrt{-4k_{off}^{ADP}k_{rot} + (k_{off}^{ADP} + k_{on}^{ADP}[\mathrm{ADP}] + k_{rot})^2}\}/2$$

$$\varepsilon = \frac{100\alpha k_{TS}k_{off}^{ADP}}{(\beta-\alpha)(\delta-\gamma)(\alpha-\gamma)(\alpha-\delta)(\beta-\gamma)(\beta-\delta)}$$

The dwell time distribution corresponds to the differentiation of $[ATP \cdot F_1{}^*]$, *i.e.* k_{rot} $[ATP \cdot F_1^{\#}]$. The histograms were fitted with the following function (*15) as shown in Fig.S1: green lines.

$$\frac{d[ATP \cdot F_1{}^*]}{dt} = C\varepsilon\{(\delta-\gamma)(\beta-\gamma)(\beta-\delta)e^{\alpha t} + (\delta-\gamma)(\alpha-\gamma)(\alpha-\delta)e^{\beta t} + (\beta-\alpha)(\alpha-\delta)(\beta-\delta)e^{\gamma t} + (\beta-\alpha)(\alpha-\gamma)(\beta-\gamma)e^{\delta t}\} \quad (*15)$$

$*\ C$: an arbitrary constant

The determined $k_{\mathrm{on}}{}^{\mathrm{ADP}}$ were 7.6 x 10^4 $\mathrm{M}^{-1}\mathrm{s}^{-1}$ for 2mM, 5mM, and 10mM ADP. The experimental data could not be fitted well with this Scheme.

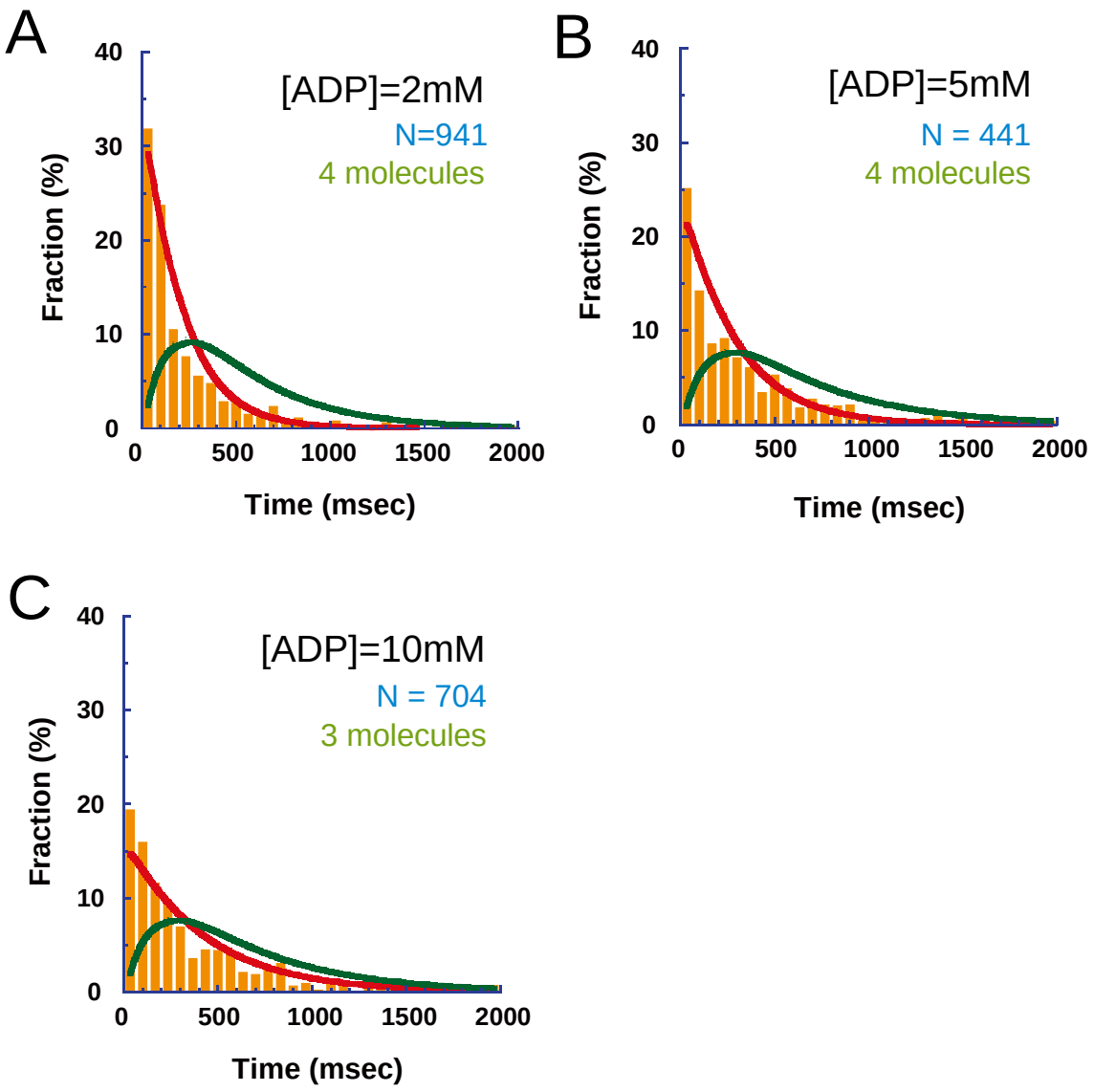

Fig. S1. Comparison with simulation. Histograms of the dwell time at 1 mM ATP in the presence of 2 mM ADP (*A*), 5 mM ADP (*B*), or 10 mM ADP (*C*) were reproduced according to Scheme 1 (red lines) or fitted by curves according to Scheme 2 (green lines). In scheme 1, ADP release was assumed to be the TS reaction, while it was not in Scheme 2.

2. Histograms of the dwell time for the pause before substep at 1 mM ATPγS at 4°C

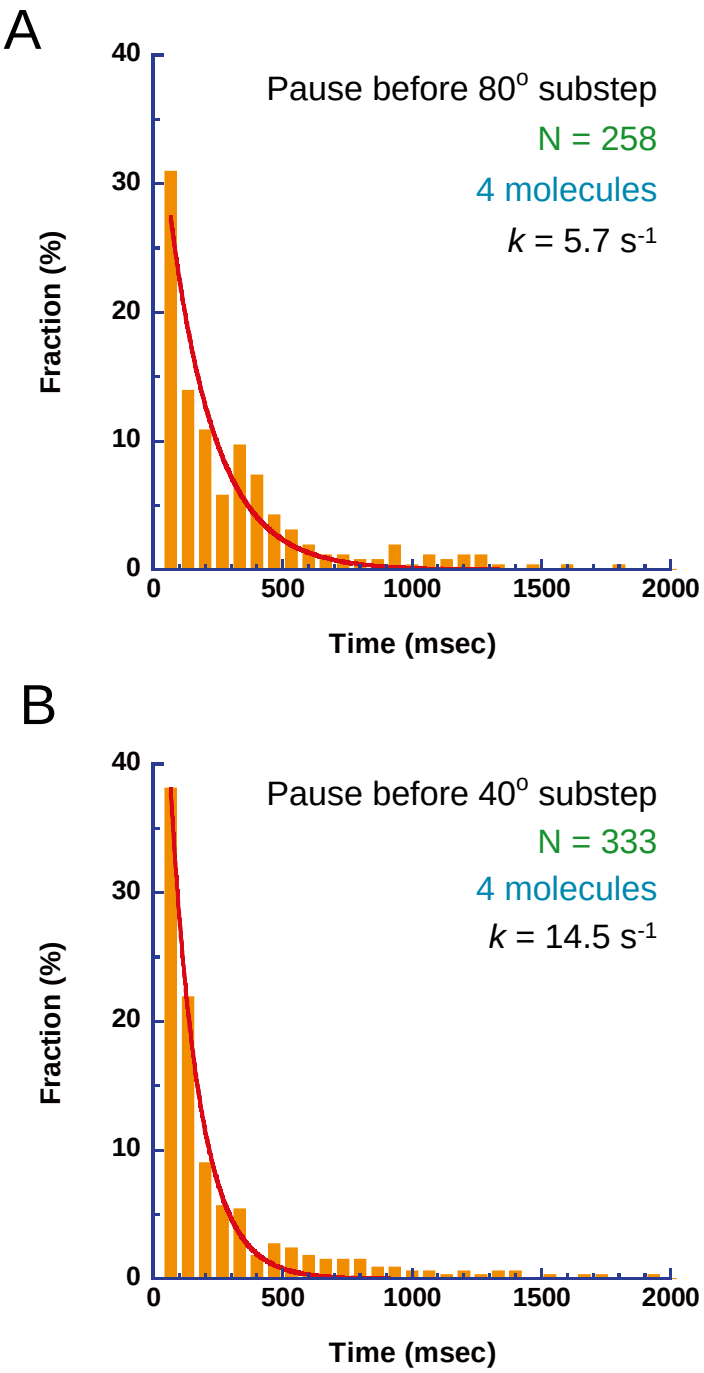

Fig. S2. Histograms of the dwell time for the pause before 80° (*A*) and 40° (*B*) substeps at 1 mM ATPγS at 4°C. Rate constants of the reaction governing the dwell time distribution were determined to be 5.7 s^{-1} (*A*) and 14.5 s^{-1} (*B*) by the curve fitting with; const.× exp (–*kt*) (red lines).

3. Effect of ADP or P_i on the rotational rate of F_1 at 4°C

Measurement of ATP hydrolysis activity in solution in the presence of ADP - ATP hydrolysis by F_1 (final 1.6 μM) was initiated by mixing with ATP (final 1 mM) in the presence of various concentration of ADP, and quenched by acid-denaturation of F_1 by perchloric acid (final 1.2%) at 40, 60, 80 and 100 sec. Procedures described above were carried out in a cold room where temperature was set to 4°C. The acid-quenched solution was centrifugated at 15,000 rpm at 4°C for 10 min, and supernatant was neutralized by K_2CO_3 (final 150mM). After neutralization, the supernatant was diluted ten times with water, and ATP hydrolysis activity was determined by measuring the concentration of P_i with BIOMOL GREEN reagent (Biomol International).

Measurement of ATP hydrolysis activity in solution in the presence of P_i - The ATP hydrolysis activity of F_1 in solution in the presence of P_i at 4°C was measured using an ATP-regenerating system as described in the Methods section.

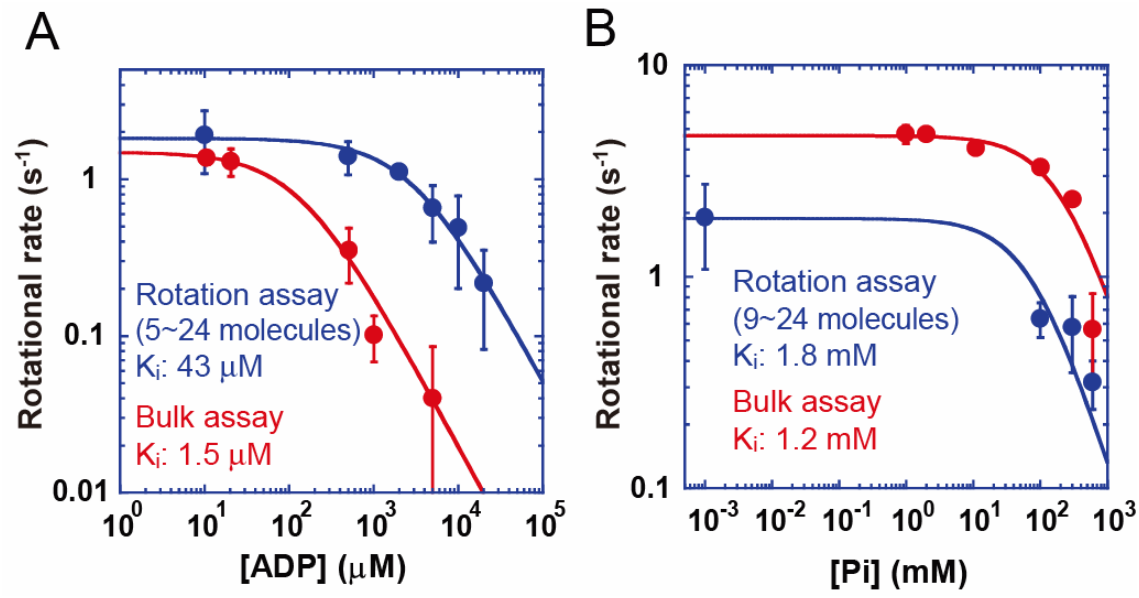

Fig. S3. Rotational rate at 1mM ATP in the presence of various concentrations of ADP (*A*) or P_i (*B*) at 4°C. Red circles are the rotational rates in free solution. Blue circles are the rational rates determined from at least nine rotating molecules of the rotation-assay. The data were fitted with a curve according to a conventional competitive inhibition scheme: $v = (V_{max} \times [ATP])/\{[ATP] + K_m (1 + [ADP \text{ or } P_i]/K_i)\}$. Concentration of ATP was 1 mM and the K_m value was set as 11.7 μM according to the data in Fig. 2A. From the fitting curves, K_i values for rotation assay and bulk assay in free solution were determined to be 43 μM, 1.5μM for ADP and 1.8 mM, 1.2 mM for P_i, respectively.

4. Rotation in the presence of excess amount of P_i at 4°C.

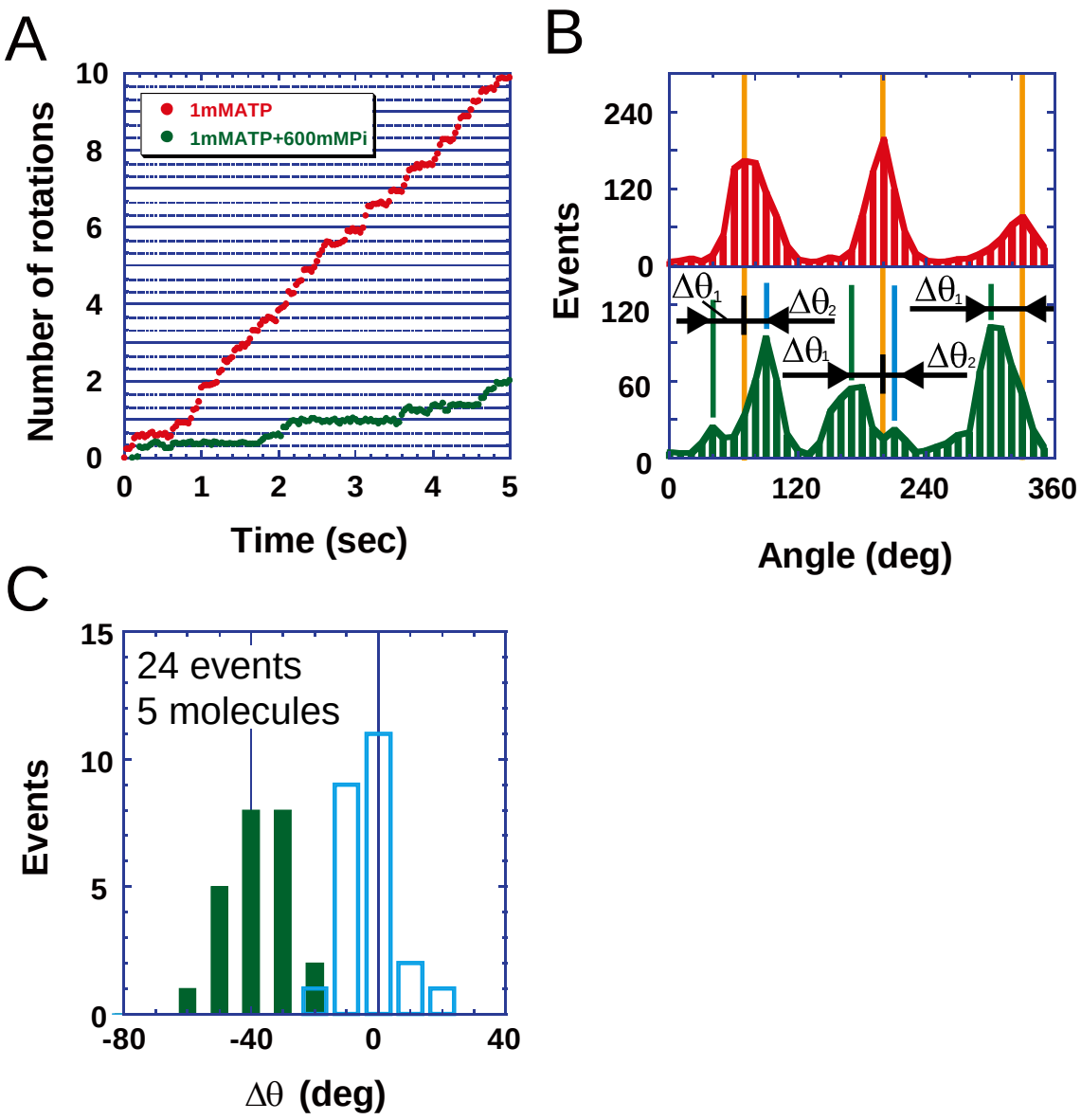

Fig. S4. Rotation in the presence of excess amount of P_i at 4°C. *A*, traces of rotation of a single F_1 molecule at 1 mM ATP with different P_i concentration. The 1mM ATP (red) buffer was replaced by the 1 mM ATP + 600 mM P_i buffer (green). *B*, histograms of angle from traces in *A*. *C*, Histogram of the displacements of the pause angle for P_i-sensitive reaction ($\Delta\theta_1$) or TS reaction ($\Delta\theta_2$) at 1 mM ATP + 600 mM P_i (lower histogram in *B*) from that for TS reaction at 1mM ATP (upper histogram in *B*) as a reference. Green and light blue bars represent distributions of $\Delta\theta_1$ and $\Delta\theta_2$, respectively.

5. Stability of F_1 complex at 4°C assessed by size-exclusion chromatography

Size-exclusion chromatography was carried out with Superdex200 10/300 GL column on ÄKTApurifier 10 (GE Healthcare). For experiment at 4°C, the column was immersed in iced water. Temperature of iced water was monitored using a thermocouple probe. To assess the dissociation of F_1 complex, the elution profile of the β subunit monomer was also examined.

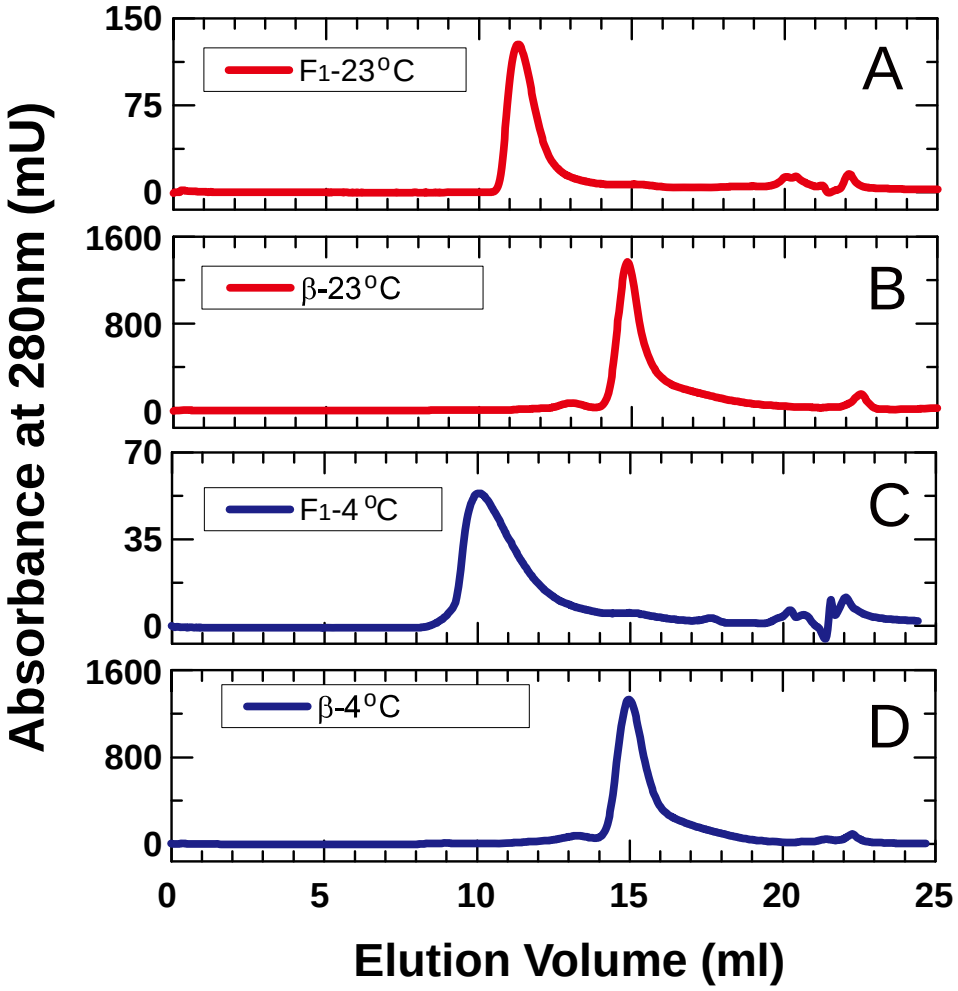

Fig. S5. Elution profiles of F_1 ($\alpha_3\beta_3\gamma$ sub-complex, *A*, *C*) and the β subunit monomer (*B*, *D*) by size-exclusion chromatography at 23°C (*A*, *B*) and 4°C (*C*, *D*). The main peak in each profile corresponds to the F_1 or the β monomer. Elution rate was set at 0.5 ml/min.

6. Stability of F_1 complex at 4°C assessed by rotary potential during the pause

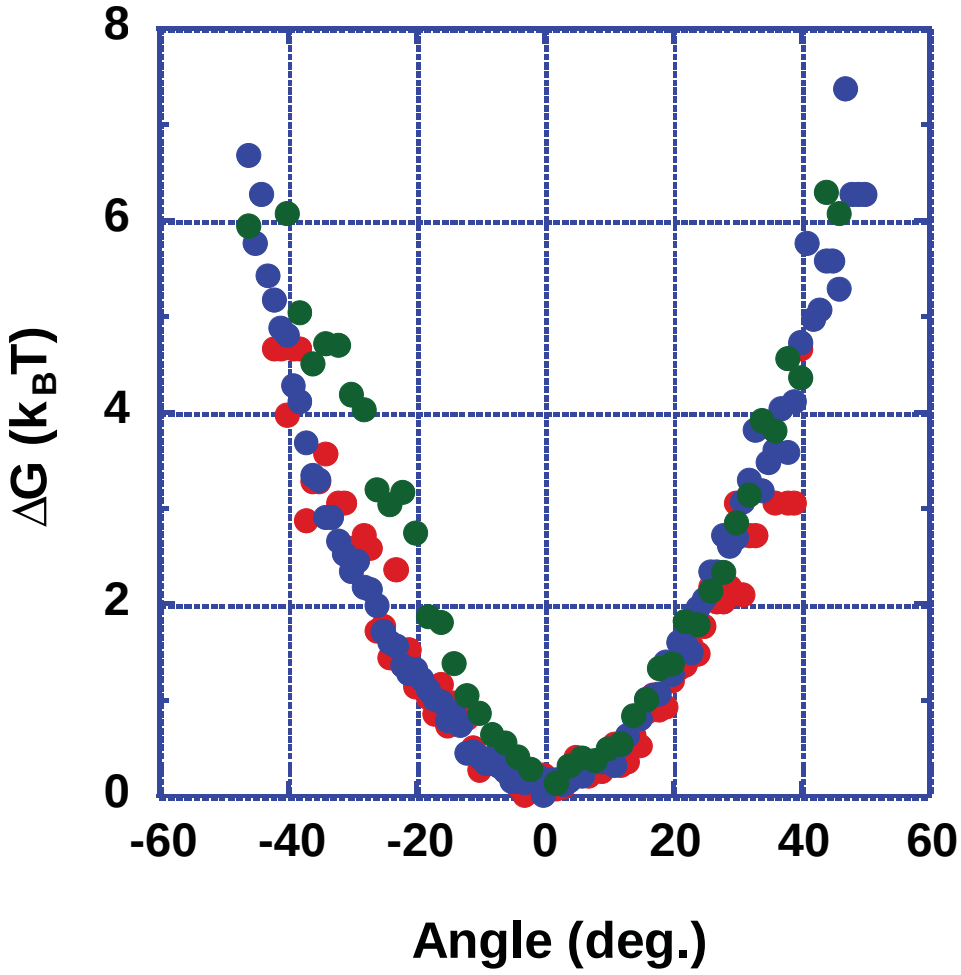

Fig. S6. Rotary potential of the F_1. Probability density of the angle of the magnetic beads during the pauses at 1 mM ATP at 4°C (red, TS reaction), at 200 nM ATP at 23°C (blue, ATP waiting) and that of ADP-inhibited F_1 at 23°C (green) were transformed into potential according to the Boltzmann distribution law. Images of the beads were recorded at 30 frames/sec with the exposure time of 1 ms (red and blue) or 2 ms (green).